0273-2289/03/109/0015/$20.00

Modeling of Anaerobic Degradation of Solid Slaughterhouse Waste

Inhibition Effects of Long-Chain Fatty Acids or Ammonia

L. Y. Lokshina,[1] V. A. Vavilin,*[,1] E. Salminen,[2] and J. Rintala[2]

[1]Water Problems Institute, Russian Academy of Sciences, Gubkina str. 3, 11991, Moscow, Russia, E-mail: vavilin@aqua.laser.ru; and [2]Department of Biological and Environmental Science, University of Jyväskylä, P.O. Box 35, FIN-40351 Jyväskylä, Finland

Abstract

The anaerobic bioconversion of solid poultry slaughterhouse wastes was kinetically investigated. The modified version of <METHANE> simulation model was applied for description of experimental data in mesophilic laboratory digester and assays. Additionally, stages of formation and consumption of long chain fatty acids (LCFA) were included in the model. Batch data on volatile solids, ammonium, acetate, butyrate, propionate, LCFA concentrations, pH level, cumulative volume, and methane partial pressure were used for model calibration. As a reference, the model was used to describe digestion of solid sorted household waste. Simulation results showed that an inhibition of polymer hydrolysis by volatile fatty acids and acetogenesis by NH_3 or LCFA could be responsible for the complex system dynamics during degradation of lipid- and protein-rich wastes.

Index Entries: Ammonia; anaerobic digestion; inhibition; long-chain fatty acids; poultry slaughterhouse waste; model; sorted solid household waste.

Introduction

Anaerobic degradation of complex organic materials is a multistep process in which hydrolysis, acidogenesis, acetogenesis, and methanogenesis are the major stages. Depending on the characteristics of the waste, any of these stages may be affected by toxicity. Poultry slaughterhouses produce high amounts of lipid- and protein-rich wastes *(1)*. The lipids included in wastes are composed mainly of neutral fats and long-chain fatty acids (LCFA). Intermediate products of lipid degradation such as

*Author to whom all correspondence and reprint requests should be addressed.

LCFA and volatile fatty acids (VFA) may accumulate in inhibitory concentrations if not effectively removed. The inhibitory effect of LCFA on a methanogenic population has been investigated in many studies. It has been stated that high LCFA contents can destabilize anaerobic digesters owing to inhibition of syntrophic acetogenic and methanogenic bacteria *(2–8)*. However, the characteristics of the inhibition of LCFA in anaerobic digestion have not been clarified yet. In protein degradation, ammonia is formed, the nonionized form of which can be inhibitory for acetogenic and methanogenic bacteria. Review of the literature shows that, generally, a level of 80 mg of N/L of free ammonia has been proposed as the minimum inhibitory level *(9,10)*. Total ammonia concentration >1500 mg/L was inhibitory at pH levels above 7.4 *(11)*.

Hydrolysis is normally considered as rate-limiting step if the substrate is in particulate form *(12)*. VFA inhibition of polymer hydrolysis has been proposed as an important regulatory mechanism of anaerobic digestion *(13,14)*. Lay et al. *(15)* reported different rates of polymer hydrolysis of lipids, proteins, and carbohydrates. Attempts to clarify the regulation mechanisms of protein- and lipid-rich substrate degradation have been made using mathematical modeling *(16,17)*. Recently, a generic anaerobic digestion model (Anaerobic Digestion Model No. 1 [ADM1]) was developed *(18)*. Nevertheless, many uncertainties in understanding the regulation mechanisms of anaerobic digestion arise when one deals with a complex substrate. LCFA inhibition can have a significant impact on process operation with lipid-rich waste, and the ADM1 cannot describe reactor behavior under high LCFA concentrations when carbon chain length changes.

The objective of the present study was to investigate the regulation mechanisms and factors potentially affecting the dynamics of anaerobic digestion of solid poultry slaughterhouse wastes (SSW) in a mesophilic batch digester and assays. Different initial waste concentration and the waste-to-inoculum ratios were modeled. As a reference, the model was used to describe digestion of solid sorted putrescible household waste (SHW).

Materials and Methods

Model

A modified version of the <METHANE> model presented here is based on the earlier developed model *(19,20)*. It is assumed in the model that SSW and SHW (initial complex substrate X_1) are mixtures of proteins (*P*), lipids (*L*), and carbohydrates (*C*). Hydrolysis, acidogenesis, acetogenesis, and methanogenesis conducted by the different groups of microorganisms were described (Fig. 1). In Fig. 1, the rectangles denote variables of the model and circles crossed denote stages of anaerobic digestion. The following groups of variables and equations are included in the model:

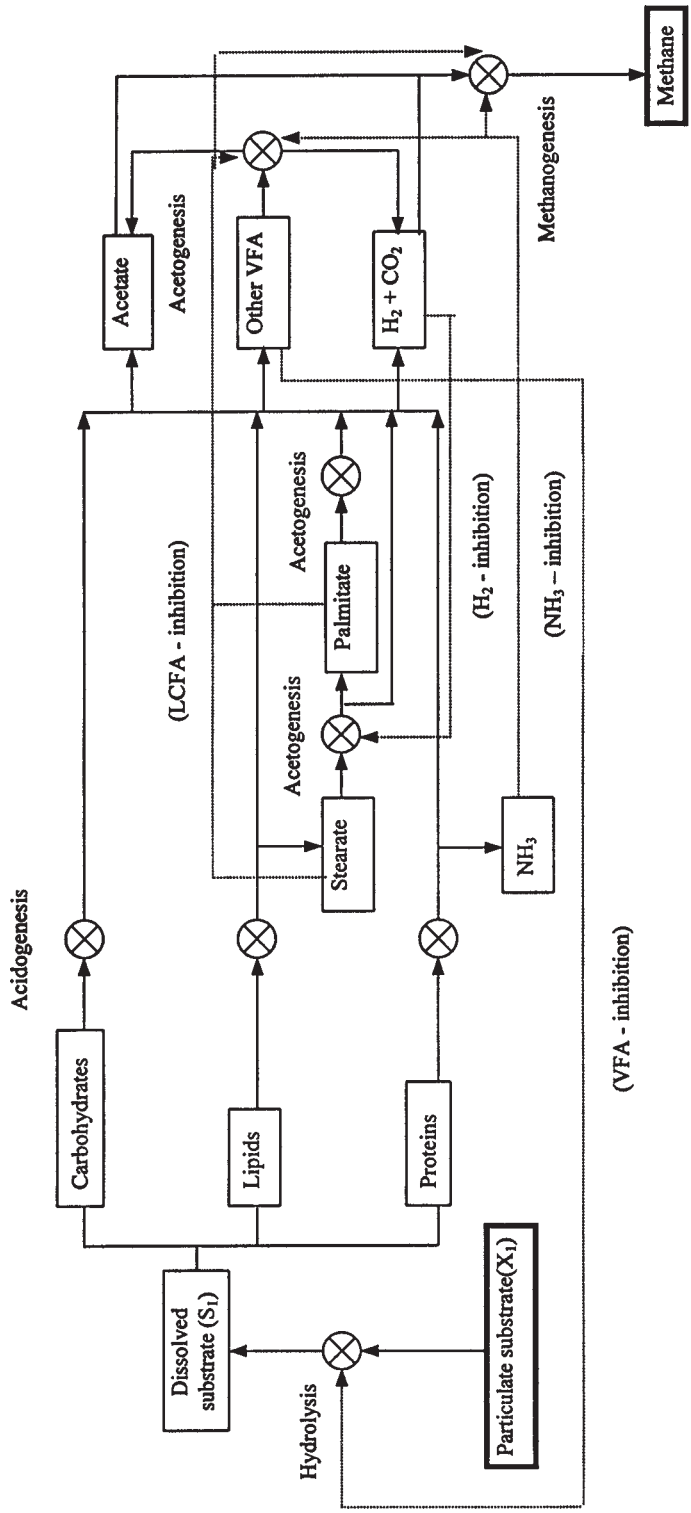

Fig. 1. Main pathways of organic component flow used in new version of <METANE> model.

1. Suspended solid concentrations (X_k, $k = 1, 2, 3$)

$$V \cdot \frac{dX_k}{dt} = q_f \cdot X_{Fk} - q_{BX} \cdot X_k + V \cdot \rho_{Xk} \quad (1)$$

in which X_{Fk} are the influent concentrations of components of suspended solids, q_f is the feed flow rate, q_{BX} is the discharge rate of excess suspended solids including biomass, ρ_{Xk} are the rates of transformation of the components of suspended solids, and V is the volume of liquid phase.

2. Active biomass concentrations (B_i, $i = 1, 2, \ldots, 10$)

$$V \cdot \frac{dB_i}{dt} = q_f \cdot B_{Fi} - q_{BX} \cdot B_i + V \cdot \rho_{Bi} \quad (2)$$

in which B_{Fi} are the influent concentrations of active bacteria, and ρ_{Bi} are the growth rates of various subpopulations.

3. Dissolved substrate concentrations (S_j, $j = 1, 2, \ldots, 13$)

$$V \cdot \frac{dS_j}{dt} = q_f \cdot \left(S_{Fj} - S_j\right) + V \cdot \rho_{Sj} + TRS_j \quad (3)$$

in which S_{Fj} are the influent concentrations of soluble substrates, ρ_{Sj} are the rates of transformation of the components of soluble substrate, and TRS_j are the rates of mass exchange between gaseous and liquid phases.

4. Partial gas pressures (p_l, $l = 1, \ldots, 5$)

$$\frac{dP_l}{dt} = \frac{RT}{V^g} \cdot \left(-TRS_l + \sum_n TRS_n \cdot \frac{P_l}{P_T}\right) \quad (4)$$

in which R is the universal gas constant, T is the temperature (°K), V^g is the volume of gas phase, and P_T is the total gas pressure.

Four variables were added to the new version of the <METHANE> model: two groups of microorganisms (stearate and palmitate consumers) and two dissolved substrates (stearic and palmitic acids).

The rate of the main limiting substrate transformation by the ith group of bacteria (ρ_{BSi}) was expressed as a product of several functions:

$$\rho_{BSi} = \rho_{mi} \cdot FT_i \cdot FL_i \cdot FI_i \cdot B_i \quad (5)$$

in which ρ_{mi} is the maximum specific rate of limiting substrate consumption by the ith group of microorganisms under optimum conditions with the biomass concentration B_i; and FT_i, FL_i, and FI_i are the functions describing the temperature dependence, mechanism of substrate limitation, and inhibition, respectively. Note that $\rho_{mi} = \mu_{mi}/Y_i$, in which μ_{mi} is the maximum specific rate of biomass growth of ith group of bacteria and Y_i is the corresponding yield coefficient.

Inhibition processes by nonionized VFA and ammonia (NH_3), LCFA, and hydrogen (H_2) were taken into consideration. The inhibiting impact of the level of NH_3, VFA, and LCFA is described by the following expression:

$$FI_i(I) = \frac{1}{1 + (I/K_{I1})^{\ln(99)}/\ln(K_{I2}/K_{I1})} \tag{6}$$

in which I is the inhibition agent concentration; and K_{I1} and K_{I2} are the inhibition constants for which process rate decreases twice and 100 times, respectively. Note that at $K_{I2} = 99K_{I1}$, the function 6 transforms into the traditional function of noncompetitive inhibition. The inhibiting impact of the hydrogen level was given by the function

$$FI_i(H_2) = \frac{1}{1 + (P_{H_2}/K_{IHi})^4} \tag{7}$$

in which P_{H2} is the partial pressure of hydrogen, and K_{IHi} is the constant of hydrogen inhibition. Because hydrogen is the very quick variable in the model, the function 7 with a power equal to 4 gives a sharp drop in activity of corresponding bacteria when hydrogen level exceeds a threshold value.

The traditional Monod dependence describing a substrate limitation was used for acidogenic, syntrophic, and acetotrophic methanogenic bacteria. For hydrogen-consuming methanogens, the resulting hydrogen consumption rate was determined using a minimum from two Monod functions for hydrogen and carbon dioxide as the limiting substrates.

First-order kinetics with inhibition by nonionized VFA was applied for the description of the hydrolysis of particulate organic matter. On the basis of experimental determinations, household waste consists of 19.5% proteins, 9.9% lipids, and 70.6% carbohydrates, and slaughterhouse waste consists of 50% proteins, 31.4% lipids, and 18.6% carbohydrates. Acidogenesis of various fractions of substrate was described by the following equations, which were selected after model calibration:

Proteins:

$$C_{16}H_{30}O_8N_4 + 5.4 \cdot H_2O = 2.8 \cdot C_2H_4O_2 + 0.1 \cdot C_3H_6O_2 + 2.1 \cdot C_4H_8O_2 + 0.1 \cdot H_2 + 1.7 \cdot CO_2 + 4 \cdot NH_3 \tag{8}$$

Lipids:

$$C_{47}H_{96}O_9 + 32 \cdot H_2O = 10.5 \cdot C_2H_4O_2 + 5.0 \cdot C_3H_6O_2 + 2.0 \cdot C_4H_8O_2 + 36.0 \cdot H_2 + 3.0 \cdot CO_2 \tag{9}$$

or

$$C_{47}H_{96}O_9 + 3.5 \cdot H_2O = 1.75 \cdot C_2H_4O_2 + 2.5 \cdot C_3H_6O_2 + 2.0 \cdot C_{18}H_{36}O_2 + 4.5 \cdot H_2 \tag{10}$$

Carbohydrates:

$$C_6H_{12}O_6 = 1.3 \cdot C_2H_4O_2 + 0.2 \cdot C_3H_6O_2 + 0.5 \cdot C_4H_8O_2 + 0.4 \cdot H_2O + 0.4 \cdot H_2 + 0.8 \cdot CO_2 \quad (11)$$

Acetogenesis of LCFA (stearic and palmitic acids) was described by the equations:

$$C_{18}H_{36}O_2 + 2 \cdot H_2O = C_{16}H_{32}O_2 + C_2H_4O_2 + 2 \cdot H_2 \quad (12)$$

$$C_{16}H_{32}O_2 + 6 \cdot H_2O = C_4H_8O_2 + 6 \cdot C_2H_4O_2 + 6 \cdot H_2 \quad (13)$$

In the model, for simplicity the stearate concentration was calculated as the sum of stearate and oleate concentrations; the palmitate concentration was considered as the sum of palmitate and myristate concentrations. The stoichiometric reactions describing butyrate and propionate degradation, and methanogenesis from acetate and H_2/CO_2, can been found elsewhere *(21)*. Visual model calibration at which the differences between the values of observed and predicted variables were close to a minimum was used.

Usually, the pH level was calculated taking into account the main buffer systems *(22)*. However, in this study the proposed model could not predict the pH dynamics correctly. Thus, a step-by-step approximation of experimental pH data was used to describe pH level.

Two possible types of inhibition were considered in the model: (1) acetogenesis (from propionate and butyrate) and acetoclastic methanogenesis inhibition by NH_3; and (2) acetogenesis (from propionate and butyrate) and acetoclastic methanogenesis inhibition by LCFA, and stearic acid degradation inhibition by H_2. Polymer hydrolysis inhibition by VFA (propionate and butyrate) was considered for both cases (Fig. 1). Traditionally, VFA or pH inhibition of hydrolysis are taken into account *(13,23)*. In the case with SSW, the pH values remained between 6.8 and 7.5. Evidently, these pH values were not inhibitory for SSW hydrolysis. In the case with SHW, the inhibitory acidic pH of 6.0 was seen during hydrolysis/acidogenesis. Using an inhibition of polymer hydrolysis by nonionized VFA, a combined effect of pH and VFA was taken into account.

Description of Experiments

Poultry slaughterhouse waste (SSW) and experimental analysis have been previously described in detail *(17)*. Preliminary minced sorted household solid waste (SHW) was from the Mustankorkea waste treatment plant (Jyväskylä, Finland). Sludge from a mesophilic (35°C) digester in a municipal sewage treatment plant (Viinikka, Tampere, Finland) was used as inoculum in all the studies.

The batch digester experiments operated at 35°C were carried out in two identical static acrylic digesters, each with a total capacity of 3 L and a liquid volume of 2 L. The gas produced in the digesters was collected in gas sampling bags. A total of 1834 mL (19.3 g of volatile solids [VS]/L) of the

inoculum was added to each digester. For startup, 150 g of SSW (19.5 g of VS/L) and 166 g of SHW (18.7 g of VS/L) were added to the digesters. The digesters were diluted with distilled water to a volume of 2 L. The initial pH of the digester's contents was 7.2 and 7.4 for the digesters with SSW and SHW, respectively. Digester content removed for sampling was taken into account in the calculations.

The batch assays were carried out in 118-mL vials with a liquid volume of 50 mL. The waste mixture, 0.75 g/vial (3.9 g of VS/L) or 1.50 g/vial (7.8 g of VS/L), was added to the vials. Inoculum (20 or 40 mL) (8.4 or 16.8 g of VS/L) was also transferred to the vials. Distilled water was added to complete the volume of 50 mL. The vials were flushed with N_2/CO_2 (80%/20%) and sealed with butyl rubber stoppers and aluminum crimps. Finally, $Na_2S{\cdot}9H_2O$ (0.25 g/L) was added to remove any residual O_2. The vials were incubated in shaken cultures at 35°C. All the assays were performed using six replicates of which three vials were sacrificed for analyses during the incubation. No extra nutrients and vitamins were added in any of the assays. Assays with four types of initial conditions were performed: 3.9 g of VS/L of waste, 8.4 g of VS/L of inoculum; 3.9 g of VS/L of waste, 16.8 g of VS/L of inoculum; 7.8 g of VS/L of waste, 8.4 g of VS/L of inoculum; 7.8 g of VS/L of waste, 16.8 g of VS/L of inoculum. Experimental error of VFA and LCFA was about 10% and not greater than 20%, correspondingly. Some modeling results of batch assays have been previously published *(17)*.

Results and Discussion

Batch Digesters

About the same amount of the substrate as VS was used in both the SSW and SHW digesters. Both wastes produced a high amount of methane, and the degree of material degradation was high and approximately equal. The ratio of substrate VS/inoculum VS was approximately equal to 1.0. A high initial concentration of proteins contained in SSW causes the high current concentration of ammonia in the reactor. Since the concentrations of LCFA were not measured in the experiments, it was impossible to determine its role in the regulation processes. Thus, VFA inhibition of hydrolysis and NH_3 inhibition of acetogenesis and methanogenesis from acetate was tested first. For the acidogenesis step of lipid degradation, Eq. 9 was used as the stoichiometric reaction.

In Figs. 2 and 3, the system dynamics in both digesters are shown. The model fitted the experimental data reasonably well. The kinetic coefficients obtained as a result of model calibration are summarized in Table 1. Evidently, the set of parameteric values obtained after model calibration is not the only one. Simulation results showed that an inhibition of acetogenesis as well as acetoclastic methanogenesis by free ammonia could be responsible for the lower rate of solids conversion into methane in the

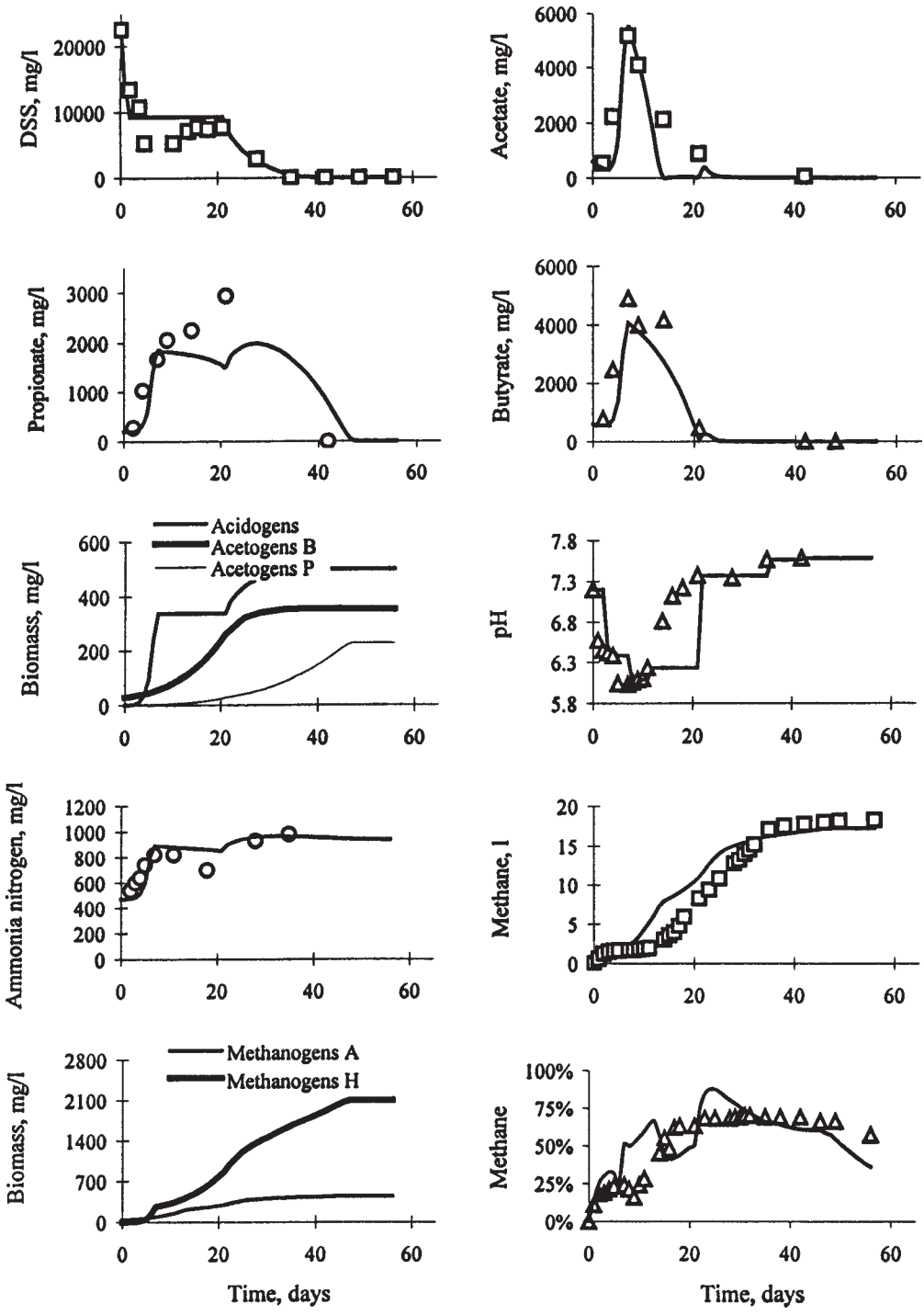

Fig. 2. Time profiles of main model variables in digester with SHW. Symbols represent experimental data; lines represent model predictions. DSS, degradable suspended solids; B, butyrate; P, propionate; A, aceticlastic; H, hydrogenotrophic.

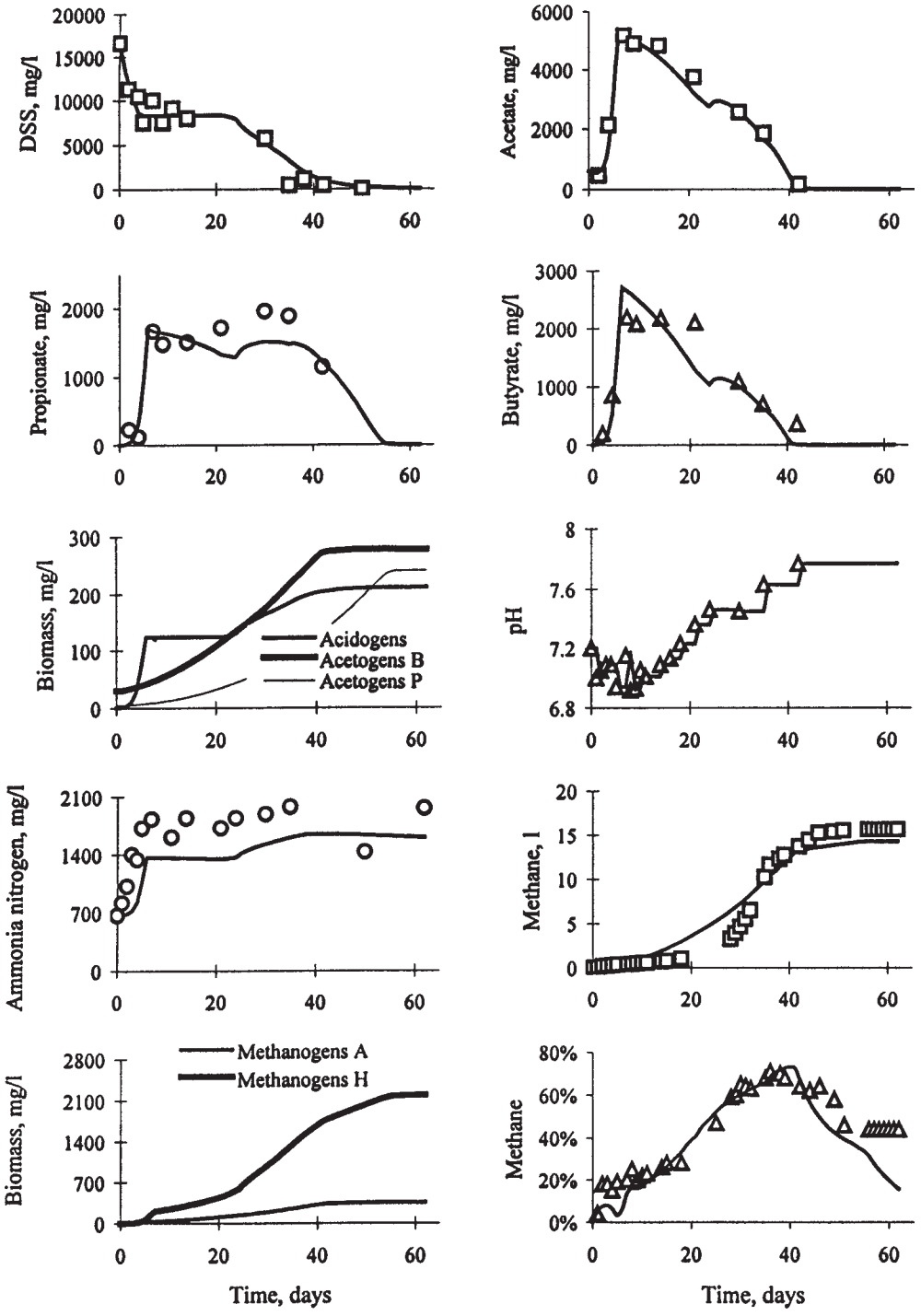

Fig. 3. Time profiles of main model variables in digester with SSW. Symbols represent experimental data; lines represent model predictions. Abbreviations are as in Fig. 2.

Table 1
Kinetic Coefficients Obtained for Batch Digestion of SSW and SHW[a]

Process[b]	X_0, B_0 (mg/L) (SSW/SHW)[c]	ρ_m (mg/[mg·d])	K_S (mg/L)	Y (mg/mg)	K_{I1}, K_{I2} (mg/L)
Hydrolysis	13,575	0.35/0.95[d]	—	—	10.05; 16.0 (VFA)
Acidogenesis	0.5/0.5	80.0	170.0	0.03	—
Acetogenesis B	30.0/28.0	5.5	20.0	0.05	15.0; 13,300.0 (NH_3)
Acetogenesis P	5.1/1.1	5.4	52.0	0.08	16.0; 13,500.0 (NH_3)
Methanogenesis A	18.1/40.1	19.3	80.0	0.02	13.5; 13,500.0 (NH_3)
Methanogenesis H	1.05/1.05	37.0	0.0012, 0.0013[e]	0.05	—

[a]NH_3 inhibition was assumed.
[b]B, butyrate; P, propionate; A, aceticlastic; H, hydrogenotrophic.
[c]X_0, B_0 are the initial concentrations of DSS and biomass of corresponding bacteria, respectively.
[d]First-order rate constant is expressed in d^{-1}.
[e]Two values of K_S for methanogenesis H corresponding to H_2 and CO_2 concentrations, respectively, are expressed in bars.

SSW reactor. An inhibition of polymer hydrolysis by nonionized VFA was proved to be important for both SSW and SHW reactors.

According to the model, the following mechanism of digestion can be suggested. The solubilization and subsequent acidification started immediately after startup in both digesters. VFA and ammonia nitrogen concentrations increased, peaking at 5.2 g/L of acetate, 6.6 g/L of other VFA, and 820 mg/L of NH_4-N in SHW and 5.2 g/L of acetate, 3.9 g/L of other VFA, and 1830 mg/L of NH_4-N on d 7 in SSW. It caused the inhibition of hydrolysis by propionate and butyrate and inhibition of acetogenesis and methanogenesis from acetate by ammonia. The rate of hydrolysis decreased approximately up to zero in both reactors but the lower concentration of ammonia for SHW caused less inhibition of acetogenesis and methanogenesis than for SSW. The lag phase in VFA consumption was substantially longer for SSW than for SHW. Biomass growth resumed the VFA consumption, which, in turn, removed hydrolysis inhibition.

The rate of polymer hydrolysis was more rapid in the SHW compared with SSW (Table 1). A slower solubilization rate of lipids compared to proteins and carbohydrates may decrease the overall rate of SSW degradation. It can be seen from Figs. 2 and 3 that the upset of polymer hydrolysis followed the intensive methanogenesis with some delay. This phenomenon was shown by Barlaz et al. *(24)* on municipal solid waste digestion.

Batch Assays

Since LCFA level was measured in the assays, it seems important to prove the assumption of inhibition of the acetogenesis and methanogenesis by LCFA. For simplicity, the total concentration of LCFA was taken into consideration as inhibiting agent. For the acidogenesis step of lipid degradation, Eq. 10 was used as the stoichiometric reaction. Results of modeling of assays 1 and 3 are shown in Figs. 4 and 5, respectively. The corresponding model parameters are presented in Table 2. The values of the maximum biomass growth rate of acetogens and methanogens ($\mu_m = \rho_m Y$) as well as the corresponding biomass yield coefficients Y were within a range presented in the literature *(18)*. According to Table 2, for the stearate-consuming acetogens, the μ_m value was substantially higher than for the palmitate-consuming acetogens (7.7 and 0.89 d^{-1}, correspondingly). From the values of inhibition constants, it may be concluded that the acetoclastic methanogenesis is inhibited by LCFA slightly in comparison with an inhibition of acetogenesis. Analysis of experimental data presented by Broughton et al. *(3)* showed a stronger inhibition by LCFA of acetogenesis than methanogenesis during anaerobic batch digestion of sheep tallow at 35°C.

The following mechanism was clarified. The solubilization and subsequent acidification began immediately after startup in all the vials. Hydrogen, VFA, and LCFA concentrations increased, peaking at 8.3 m*M* VFA (propionate and butyrate) and 4.02 m*M* LCFA on d 12 in vial 1, 9.6 m*M* VFA and 5.9 m*M* LCFA on d 3 in vial 2, 17.0 m*M* VFA on d 6 and 5.8 m*M* LCFA on d 12 in vial 3, and 17.0 m*M* VFA on d 6 and 10.9 m*M* LCFA on d 3 in vial 4.

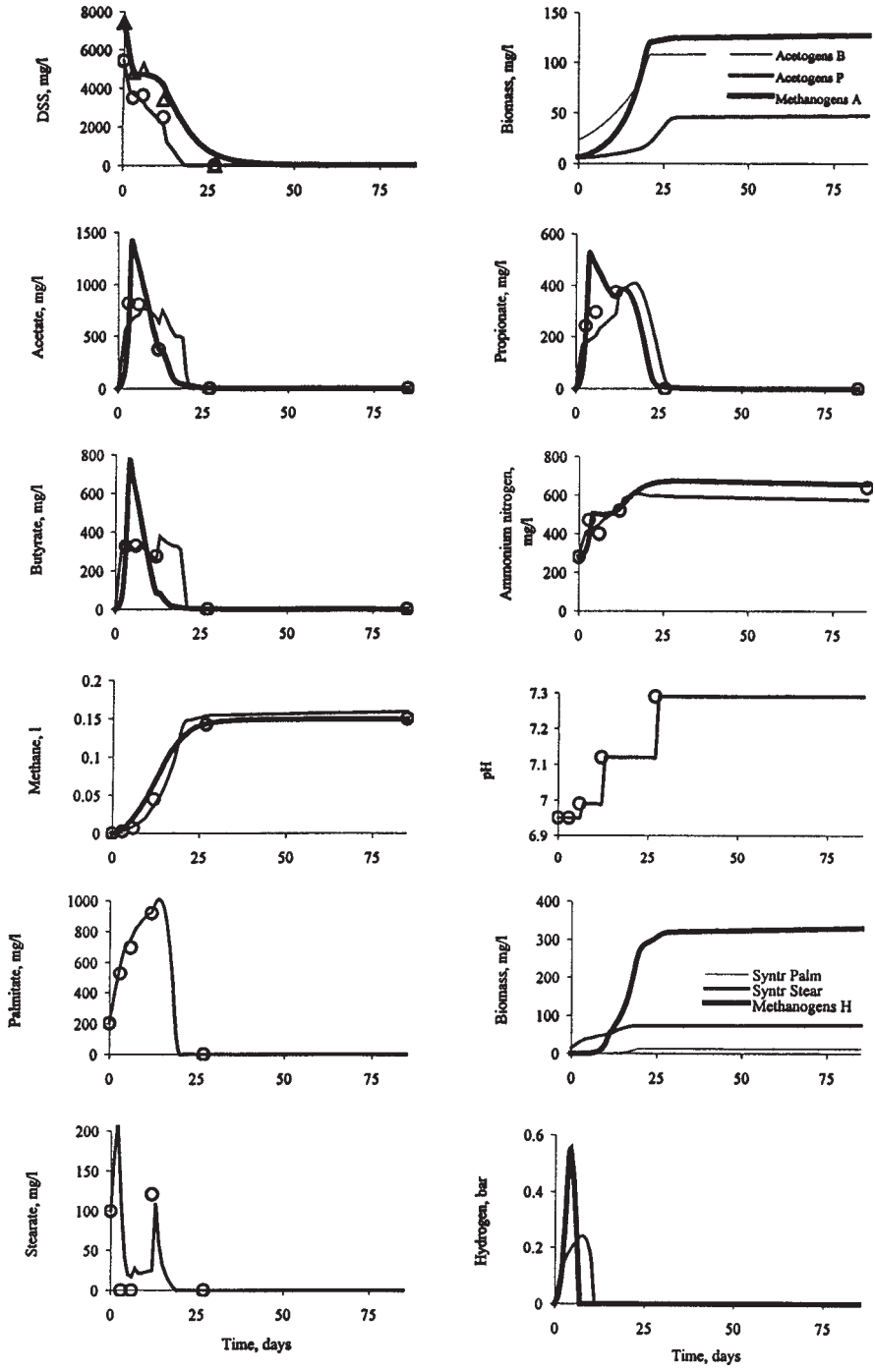

Fig. 4. Time profiles of main model variables in assay 1. Symbols represent experimental data; lines represent model predictions with LCFA (——) or NH_3 (▬▬) inhibition. Initial concentration of DSS was assumed equal to 7431 and 5030 mg/L in the simulations with NH_3 and LCFA inhibition, respectively. The ratio of degradable parts of proteins, lipids, and carbohydrates in SSW was assumed equal to 0.65:0.314:0.036. The populations dynamics as well as kinetics of stearate and palmitate correspond only to the model with LCFA inhibition. Syntr, syntrophs; Palm, palmitate; Stear, stearate. Other abbreviations are as in Fig. 2.

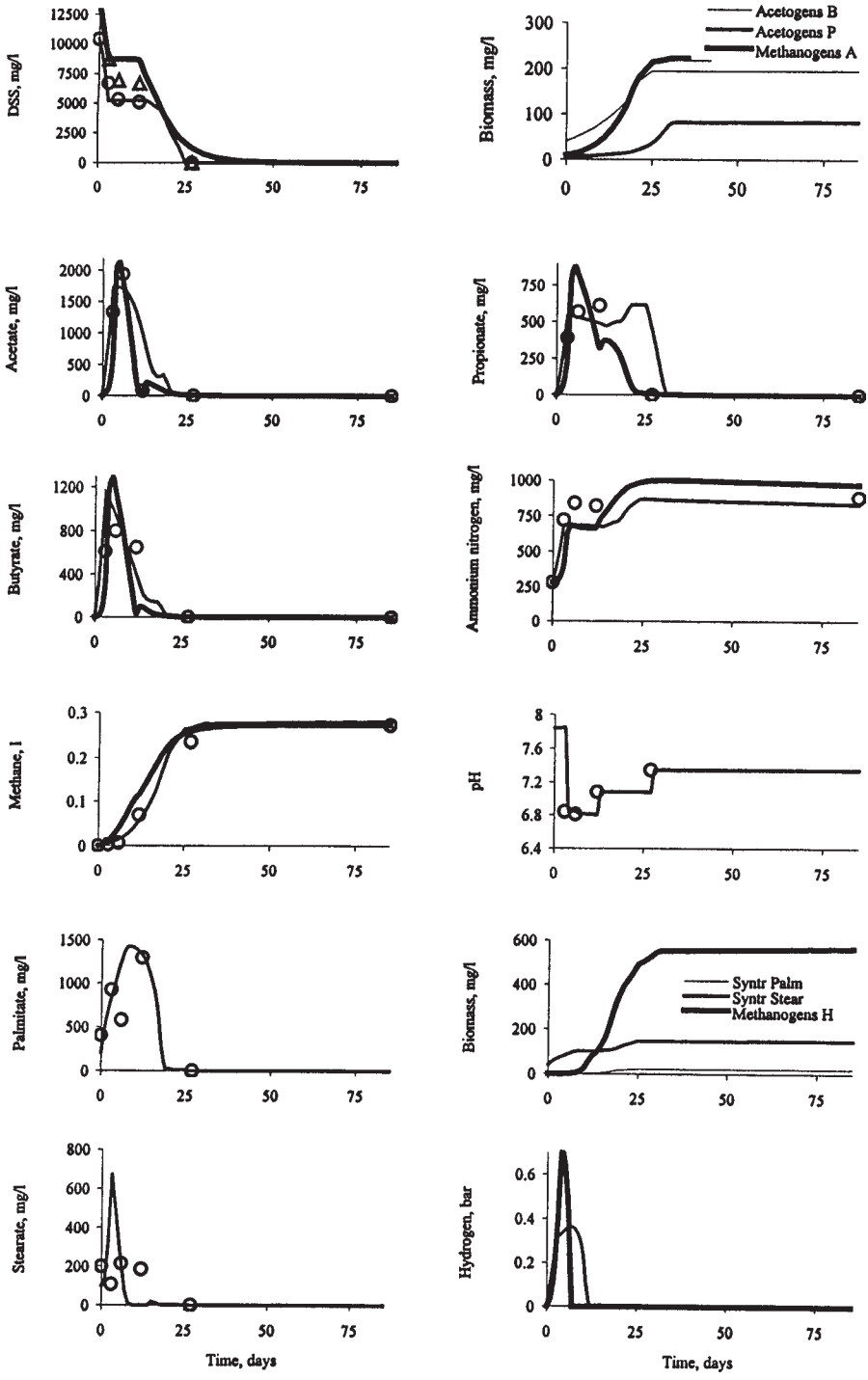

Fig. 5. Time profiles of main model variables in assay 3. Symbols represent experimental data; lines represent model predictions with LCFA (——) or NH_3 (▬▬) inhibition. The initial concentration of DSS was assumed equal to 13,560 and 9030 mg/L in the simulations with NH_3 and LCFA inhibition, respectively. The ratio of degradable parts of proteins, lipids, and carbohydrates in SSW was assumed equal to 0.60:0.364:0.036. Abbreviations are as in Figs. 2 and 4.

Table 2
Kinetic Coefficients Obtained for Four Vials[a]

Process[b]	ρ_m (mg/[mg·d])	K_S (mg/L)	Y (mg/mg)	K_{I1}, K_{I2} (mg/L)
Hydrolysis	0.7[c]	—	—	6.00; 6.05 (VFA)
Acidogenesis	159.0	170.0	0.03	—
Acetogenesis B	5.5	20.0	0.05	4.0; 9.10^5 (LCFA)
Acetogenesis P	5.4	72.0	0.08	2.0; 9.10^5 (LCFA)
Methanogenesis A	19.3	80.0	0.02	1360; 9.10^5 (LCFA)
Methanogenesis H	27.3	0.0012, 0.0013[d]	0.02	—
Acetogenesis Palm	99.7	100.0	0.009	—
Acetogenesis Stear	175.9	100.0	0.04	0.086[e] (hydrogen)

[a]LCFA inhibition was assumed.
[b]B, butyrate; P, propionate; A, aceticlastic; H, hydrogenotrophic; Palm, palmitate; Stear, stearate.
[c]First-order rate constant is expressed in d^{-1}.
[d]Two values of K_S for methanogenesis H corresponding to H_2 and CO_2 concentrations, respectively, are expressed in bars.
[e]Inhibition constant is expressed in bars.

Thus, according to the model, VFA and LCFA accumulated rapidly after polymer hydrolysis/acidogenesis; as a result, the high VFA (propionate and butyrate) concentration inhibited hydrolysis and that of LCFA inhibited acetogenesis on d 3 to 4. Quickly, the rate of hydrolysis decreases approximately up to zero. However, a decrease in butyrate concentration stops hydrolysis inhibition. The cause of earlier butyrate consumption was the rather high initial biomass concentration of acetogens consuming butyrate (acetogens butyrate). Because of low initial biomass concentration of acetogens consuming propionate (acetogens propionate), the rate of propionate production was higher than the rate of propionate consumption, and during some time propionate concentration increased slowly. Propionate and butyrate concentrations began to decrease rapidly after LCFA conversion.

In assay 1, after initial rapid accumulation, stearate began to be consumed much faster than it was produced. Thus, the stearate concentration began to drop rapidly (Fig. 4). However, the increasing level of hydrogen became inhibitory to stearate consumption (d 9). Since that time the stearate concentration increased, but, again, the stearate concentration began to fall (d 12) because the growth of hydrogenotrophic methanogens lowered the hydrogen concentration. Because of the low number of syntrophs consuming palmitate during the first 12 d, palmitate was consumed at a lower rate than produced, driving up its concentration, which began to drop on d 16 after a rapid growth of syntrophs. When the palmitate and stearate concentrations became noninhibitory to butyrate and propionate consumption, a rapid acetogenesis accompanied by a rapid hydrolysis followed, setting off a rapid methanogenesis. As it follows from the values of maximum specific rate of substrate consumption ρ_m shown in Table 2, acetogenesis from LCFA, especially from stearate, was a much more rapid process than that from butyrate and propionate. Overall, the model suggested that syntrophic LCFA degradation was the rate-limiting step in the beginning of all the assays, which is in accordance with previous observations *(3,7)*, and in the final stage of the degradation, polymer hydrolysis was the rate-limiting step. The simulation results showed that the degradation patterns include complicated feedback connections, also making the degradation process complicated.

Variation in inoculum/waste ratio does not greatly affect the system dynamics in the experiments under consideration. Probably, in the case of smaller initial biomass concentration this influence would appear more brightly. The minor influence of inoculum/waste ratio was also reported by Rinzema et al. *(7)*.

The same kinetic coefficients that we found from digester data (Table 1) were used for testing the model with NH_3 inhibition for assay data except the parameters of hydrolysis. Figures 4 and 5 show the system dynamics in assays 1 and 3 as the examples with the first-order rate constant for hydrolysis equal to 0.3 d^{-1}. It was found that the model fits all assay data reasonably well when the initial concentrations of bacteria were changed.

Note that the methane volume released must be higher if the pathway through LCFA is assumed as in the case without LCFA formation and consumption. Hence, it was necessary to assume the higher initial concentration of degradable suspended solids (DSS) in the model with NH_3 inhibition (Figs. 4 and 5).

From the experimental data, it was concluded that the lower concentration of VFA in assays than in digester inhibits hydrolysis. To make that determination, the value of K_{I1} = 5.05 mg/L of nonionized VFA was used in the model for assays (compare with the corresponding value of 10.05 mg/L for digester). The conditions of digestion, especially hydrolysis stage, may be rather different in the digester and assays. Note that the vials were mixed and were much more diluted than the digesters (see Materials and Methods). As it follows from the data, the peak levels of VFA and ammonia were less substantial in assays than in SSW digester. Thus, there was no substantial delay in methane production. Only in vial 4 did a slight ammonia inhibition take place. Finally, we can conclude that the two assumptions concerning inhibition of acidogenesis and methanogenesis by NH_3 or LCFA discussed herein demonstrate no significant differences. In the actual systems both approaches may contribute.

The pH values remained between 6.8 and 7.5 in all studies throughout the experiment despite the periodically high VFA concentrations. Apparently this was owing to a rather high ammonia concentration and ammonia–bicarbonate buffer system involved, as reported previously *(25,26)*.

Simulations of Continuous-Flow Digester

As mentioned, one of the main problems arising during lipid-contained waste digestion is strong LCFA inhibition. The results of simulations of continuous-flow digester at different retention times taking into account LCFA inhibition are presented in Fig. 6. It is clear that at HRT >15 d the effective solids removal and methane production occurred. According to the model, a long time (hundreds of days) is needed to reach a steady state. After operating the process for more than one and a half years, an increase in organic loading to 5 g of VS/L and a decrease in HRT to 22 d was obtained without accumulation of VFA *(27)*. By contrast, Salminen and Rintala *(28)* showed that in the range of 25–13 d, the process appeared inhibited; however, inhibition was reversible.

Conclusion

Simulation results showed that an inhibition of butyrate and propionate acetogenesis as well as acetoclastic methanogenesis by LCFA or free ammonia could be responsible for the lower rate of solids conversion into methane in the SSW reactor in comparison with the SHW reactor. In both reactors, a hydrolysis inhibition by high VFA values was an important feature for system dynamics. The upset of polymer hydrolysis followed the intensive methanogenesis with some delay in both digesters. According to

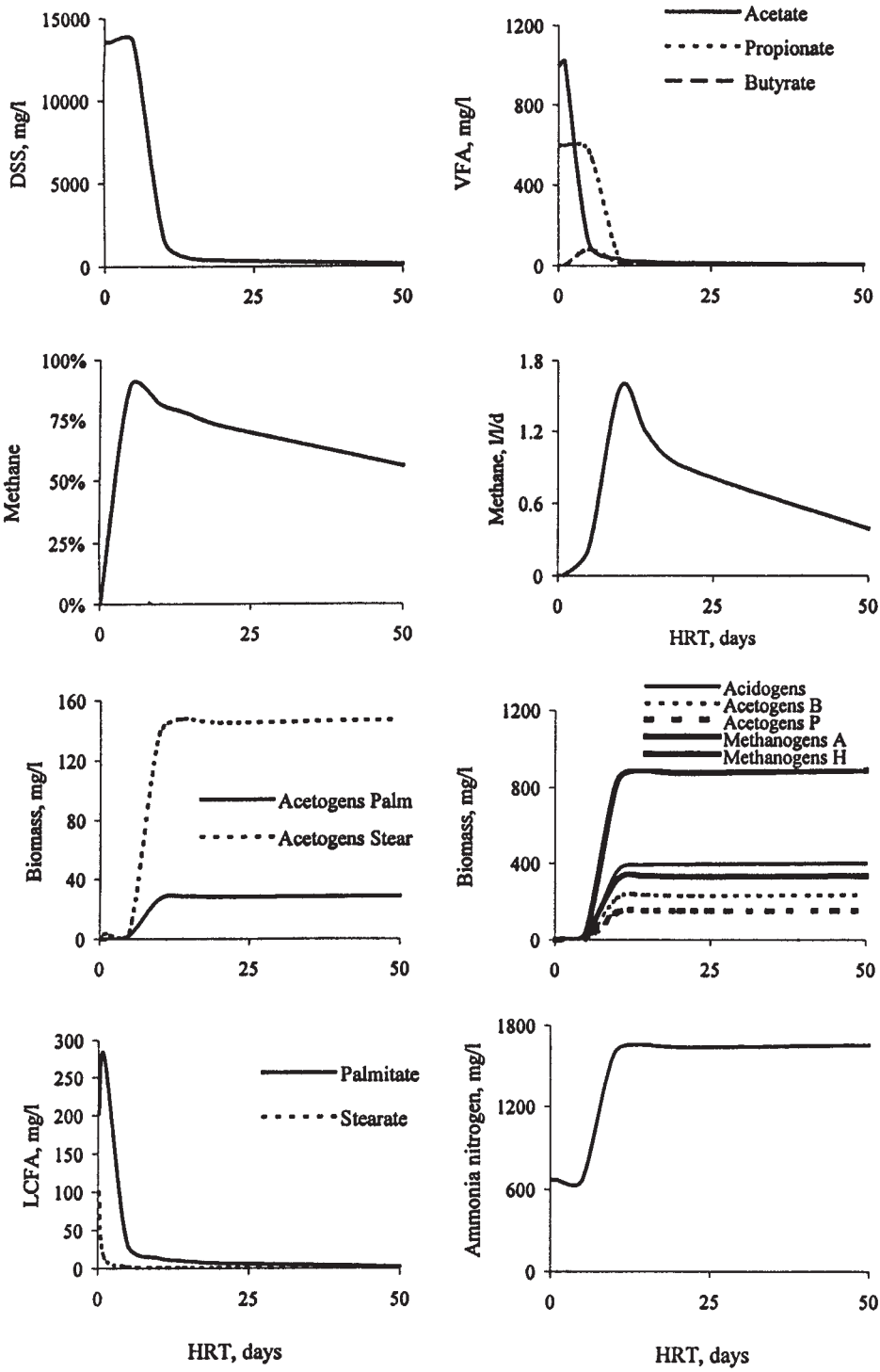

Fig. 6. Steady-state values of model variables with LCFA inhibition in continuous-flow SSW digester as function of hydraulic retention time (HRT). The influent concentration of DSS was assumed equal to 13,575 mg/L. Abbreviations are as in Figs. 2 and 4.

the model, in the assays the lower concentration of VFA inhibits hydrolysis. In continuous-flow reactor, a long time (hundreds of days) is needed to achieve a steady state.

References

1. Salminen, E. and Rintala, J. (2002), *Biores. Technol.* **83,** 15–25.
2. Angelidaki, I. and Ahring, B. K. (1992), *Appl. Microbiol. Biotechnol.* **37,** 808–812.
3. Broughton, M. J., Thiele, J. H., Birch, E. J., and Cohen, A. (1998), *Water Res.* **32,** 1423–1428.
4. Galbraith, H., Miller, T. B., Paton, A. M., and Thompson, J. K. (1971), *J. Appl. Bacteriol.* **34,** 803–813.
5. Hanaki, K., Matsuo, T., and Nagase, M. (1981), *Biotechnol. Bioeng.* **23,** 1591–1610.
6. Koster, I. W. and Gramer, A. (1987), *Appl. Microbiol. Biotechnol.* **53,** 403–409.
7. Rinzema, A., Boone, M., van Knippenberg, K., and Lettinga, G. (1994), *Water Environ. Res.* **66,** 40–49.
8. Roy, F., Samain, E., Dubourguier, H. C., and Albagnac, G. (1986), *Arch. Microbiol.* **145,** 142–147.
9. Koster, I. W. and Lettinga, G. (1984), *Agric. Wastes* **9,** 205–216.
10. De Baere, L. A., Devocht, M., van Assche, P., and Verstraete, W. (1984), *Water Res.* **18,** 543–548.
11. McCarty, P. L. (1964), *Public Works* **95,** 91–94.
12. Pavlostathis, S. G. and Giraldo-Gomez, E. (1991), *Crit. Rev. Environ. Cont.* **21,** 411–490.
13. Angelidaki, I., Ellegaard, L., and Ahring, B. K. (1993), *Biotechnol. Bioeng.* **42,** 159–166.
14. Vavilin, V. A., Rytov, S. V., Lokshina, L. Y., and Rintala, J. (1999), in *Proceedings of the 2nd International Conference on Solid Waste Anaerobic Digestion*, Mata-Alvarez, J., Tilche, A., and Cecchi, F., eds., Avda Can Sucarrats, Barcelona, June 15–18, vol. II, pp. 1–4.
15. Lay, M., Li, Yu, and Noike, T. (1998), *J. Environ. Eng.* **124,** 730–736.
16. Angelidaki, I., Ellegaard, L., and Ahring, B. K. (1997), in *Proceedings of the 8th International Conference on Anaerobic Digestion*, Sendai, May 25–29, Ministry of Education of Japan, vol. 1, pp. 245–252.
17. Salminen, E., Rintala, J., Lokshina, L. Y., and Vavilin, V. A. (1999), *Water Sci. Technol.* **41(3),** 33–41.
18. Batstone, D. J., Keller, J., Angelidaki, I., Kalyuzhnyi, S. V., Pavlostathis, S. G., Rozzi, A., Sanders, W. T. M., Siegrist, H., and Vavilin, V. A. (2002), Anaerobic Digestion Model No. 1. Scientific and Technical Report No. 13, IWA, Cornwall, UK.
19. Vasiliev, V. B., Vavilin, V. A., Rytov, S. V., and Ponomarev, A. V. (1993), *Water Resour.* **20,** 633–643.
20. Vavilin, V. A., Vasiliev, V. B., Ponomarev, A. V., and Rytov, S. V. (1994), *Biores. Technol.* **48,** 1–8.
21. Vavilin, V. A., Lokshina, L. Y., Rytov, S. V., Kotsyurbenko, O. R., and Nozhevnikova, A. N. (1998), *Biores. Technol.* **63,** 159–171.
22. Vavilin, V. A., Vasiliev, V. B., Rytov, S. V., and Ponomarev, A. V. (1995), *Water Res.* **29,** 827–835.
23. Veeken, A., Kalyuzhnyi, S., Scharff, H., and Hamelers, B. (2000). *J. Environ. Eng.* **126,** 1076–1081.
24. Barlaz, M. A., Schaefer, D. M., and Ham, R. K. (1989), *Appl. Environ. Microbiol.* **55,** 55–65.
25. Ahring, B. K., Angelidaki, I., and Johansen, K. (1992), *Water Sci. Technol.* **7,** 311–318.
26. Georgacakis, D., Sievers, D. M., and Ianotti, E. L. (1982), *Agric. Wastes* **4,** 427–441.
27. Edstrom, R., Nordberg, A., and Thyselius L. (2003), *Appl. Biochem. Biotechnol.* **109,** 127–138.
28. Salminen, E. and Rintala, J. (2003), *Water Res.* **36,** 3175–3182.